ISBN: 978-3-95450-232-5 ISSN: 2673-7000 doi:10.18429/JACoW-NAPAC2022-WEXD5

BENCHMARKING SIMULATION FOR AWA DRIVE LINAC AND EMITTANCE EXCHANGE BEAMLINE USING OPAL, GPT, AND IMPACT-T*

S.-Y. Kim†, G. Ha, J. Power, G. Chen, S. Doran, W. Liu, E. Wisniewski
Argonne National Laboratory, Lemont, IL, USA
P. Piot, E. Frame, Northern Illinois University, DeKalb, IL, USA

Abstract

At the Argonne Wakefield Accelerator (AWA) facility, particle-tracking simulations have been critical to guiding beam-dynamic experiments, e.g., for various beam manipulations using an available emittance-exchange beamline (EEX). The unique beamline available at AWA provide a test case to perform in-depth comparison between different particle-tracking programs including collective effects such as space-charge force and coherent synchrotron radiation. In this study, using AWA electron injector and emittance exchange beamline, we compare the simulations results obtained by GPT, OPAL, and IMPACT-T beam-dynamics programs. We will specifically report on convergence test as a function of parameters that controls the underlying algorithms.

INTRODUCTION TO THE AWA BEAM TEST FACILITY

A research program to develop methods to control high-brightness and high-charge beam distributions is being carried out at the AWA beam test facility [1]. The AWA facility house three RF photocathode beamlines and, the present study uses the AWA drive-beam photoinjector. The drive-beam linac consists of an L-band RF gun followed by six standing-wave cavities [2]. The beamline can produce electron bunches with charges ≤ 400 nC and energies ≤ 63 MeV. The gun is nested within three solenoid magnets (referred to as bucking, focusing, and matching solenoids) to control the beam and its transverse emittance [3]. The linac section also incorporate three solenoid magnets mostly use to focus high-charge beams. The emittance-exchange (EEX) beamline, located downstream of the drive linac section, consists of an L-band transverse deflecting cavity (TDC) flanked between two dogleg sections.

AWA's bunch control program aim at developing methods to tailor the bunch's current profile [4, 5]. An example of method used for current shaping consists in inserting a mask to transversely shape the beam upstream of the EEX and use the EEX beamline to transfer this shape in the longitudinal phase space. So far current profiles produced have successfully supported the experimental demonstration of record transformer ratio in dielectric slab and plasma [6, 7]. AWA's program in beam-manipulation techniques relies on accurate models to achieve the required precise beam shapes.

* The research at Argonne National Laboratory is funded by the U.S. DOE under contract No. DE-AC02-06CH11357.
† seongyeol.kim@anl.gov

Table 1: Global Parameters for Convergence Test

	Charge (nC)	Matching solenoid (A)	UV radius (mm)
Case 1	0.1	240	1.0
Case 2	1.0	240	2.0
Case 3	10.0	240	4.0
Case 4	50.0	230	7.0

Moreover, for the high-charge beam case, it is expected that collective effects, such as the space-charge force (SC) and coherent synchrotron radiation (CSR), will be the main sources of 6D phase space degradation. Therefore, in addition to the particle motion in a linear system, validation of the collective effects calculated by the simulation is critical. Some prior studies on benchmarking of the OPAL simulation [8] with GPT [9] and ASTRA [10] were performed but limited to the RF-gun section [11]. In this paper, we extend the benchmarking study to the full AWA beamline. We first present a convergence test of the OPAL simulation and then compare the results from OPAL, GPT, and IMPACT-T [12] for the AWA drive linac and EEX beamline.

OPAL CONVERGENCE TEST

The convergence studies consider the drive-linac beamline for bunch charges and configuration listed in Table 1.

First, we performed a parameter scan with the OPAL simulation code for the AWA drive linac section by varying global parameters *NBIN* and *EMISSIONSTEPS* [8] that impact the emission process. In all cases, the initial photocathode-laser ultraviolet (UV) pulse is considered to have a transverse uniform distribution and a Gaussian temporal profile with duration of 0.3 ps (FWHM). The bucking- and focusing-solenoid currents are both set to 550 A, and the drive-linac solenoids were not used. The phases of the gun and 6 linac accelerating cavities are tuned for maximum energy gain. The simulation time step was set to 1.0 ps in the cavities and 10.0 ps in drift spaces. It was confirmed that, in our parameter space, normalized emittance after drive linac section is converged regardless of the value of *NBIN* (setting *NBIN* = 1 is also valid for the simulations). In addition, we have checked that the emittance value was converged when *EMISSIONSTEPS* ≥ 500; in other words, the time step near the cathode should be less than 2.0 fs.

ISBN: 978-3-95450-232-5 ISSN: 2673-7000 doi:10.18429/JACoW-NAPAC2022-WEXD5

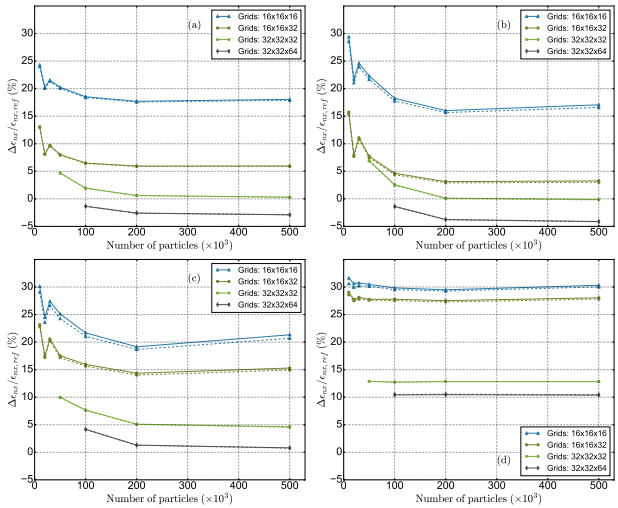

Figure 1: Emittance convergence study. $\epsilon_{nx,ref}$ is the normalized emittance obtained using the beam charge of 50 nC and grid size of 64 × 64 × 64. Beam charge is (a) 0.1 nC, (b) 1.0 nC, (c) 10.0 nC, and (d) 50.0 nC, respectively.

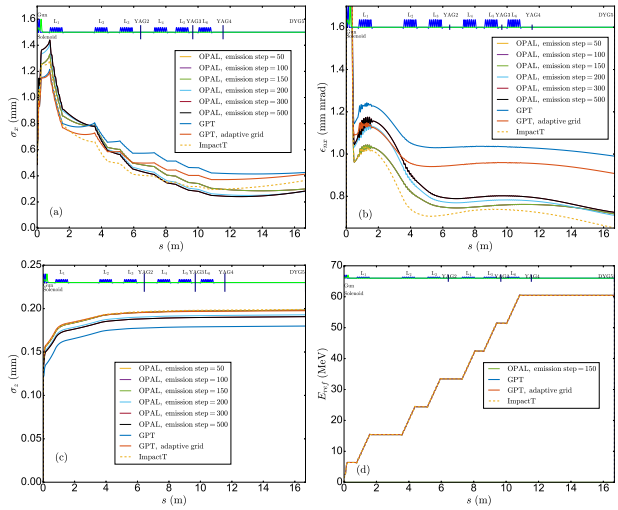

Figure 2: (a) RMS beam envelope, (b) normalized emittance, (c) RMS bunch length, and (d) average kinetic energy along the AWA drive-linac beamline.

After confirming *NBIN* and *EMISSIONSTEPS* parameters, convergence check of the OPAL simulation has been performed. Figure 1 displays the convergence results in terms of the relative emittance change $\Delta\epsilon_{nx} = \epsilon_{N\text{part,grid}} - \epsilon_{500\text{k,64}}$ where the reference emittance $\epsilon_{500\text{k,64}}$ is simulated for 5×10^5 macroparticles and $64\times64\times64$ grid cells. In the latter figure, the solid lines are obtained with the time step mentioned above, while the dashed lines were produced with a time step of 0.1 ps and 1.0 ps respectively in the cavities and drift spaces. In Fig. 1(a), the convergence is reached when the number of particles is 2×10^5 and grid size is $32 \times 32 \times 32$. The same conclusions applied to the 1.0 nC case. However, Figs. 1(c, d), suggest that the simulation results have not yet converged. Thus, for the high-charge case, further convergence test is needed with increased number of particles and grid size.

COMPARISON OF THE SIMULATION RESULTS

Space-Charge Dominated Regime: AWA Drive Linac

Following the convergence check, we set the global parameters of the OPAL simulation, and compare the results along the drive linac section with the results from GPT and Impact-T. Here, we chose the first case in Table 1; thus, the number of macroparticles in the OPAL is 2×10^5 and grid size is $32 \times 32 \times 32$. Figure 2 presents the evolution of the RMS beam envelope, normalized emittance, RMS bunch length, and average kinetic energy along the beamline. In the GPT setup, the number of macroparticles is 1×10^5. In addition there are two grid size setting: a uniform 46×46×46 mesh and an *adaptive* meshing which is automatically set for accuracy of the calculation and reduction on computation time [13]. The Impact-T model uses the same settings as OPAL except for the *EMISSIONSTEPS* set to 1500.

As can be seen in Fig. 2(d), the average kinetic energy is identical for all cases with different simulation programs. In addition, the RMS bunch length in Fig. 2(c) is similar to each other when the *EMISSIONSTEPS* in OPAL is set up to 150. As the *EMISSIONSTEPS* increases, its result deviates from the lower-value cases and from the Impact-T and GPT adaptive-mesh results. However, in Fig. 2(a), even the trend of the RMS beam envelope is not similar from the gun to the beginning of the first linac section; OPAL and Impact-T results have larger RMS beam size compared to that from GPT and the emittances agree within 30%; see Fig. 2(b).

It is expected that the deviation comes from the different calculation algorithm of the space-charge effects near the cathode [8, 13] due to small spot size, short bunch duration, and low energy. To mitigate the space charge effect and see the trend, we increased the UV laser radius to 5.0 mm the corresponding results appear in Figs. 3(a, b). Here, the RMS envelope from the OPAL is well matched with the GPT and Impact-T result. In case of the emittance, even though there is still deviation after the gun section, its trend is similar to that with GPT and Impact-T, and the final deviation from the OPAL simulation is 12%(0.3%) with respect to GPT(Impact-T). In addition, the OPAL results with the *EMISSIONSTEPS* = 500 is also in agreement with the other cases.

As the charge increases, as shown in Figs. 3(c, d), however, there is a large deviation of the envelope and emittance when *EMISSIONSTEPS* = 500 is used. Similar behavior is observed when the space charge near the cathode is expected to be large, for example, with charge of 0.1 nC and UV spot size of 1.0 mm, or charge is 50 nC. Therefore, we reduced *EMISSIONSTEPS* to be 150, and the OPAL simulation results became reasonably agreed with those from OPAL and Impact-T. Here, in case of the normalized emittance, the

ISBN: 978-3-95450-232-5 ISSN: 2673-7000 doi:10.18429/JACoW-NAPAC2022-WEXD5

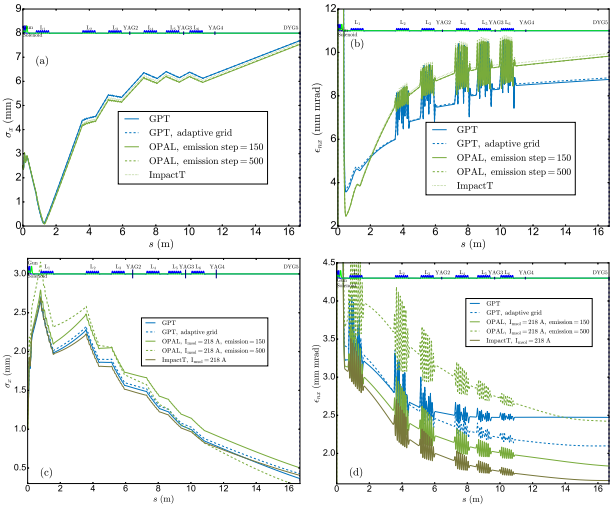

Figure 3: (a, b): RMS beam size and normalized emittance with 5.0 mm UV size where the beam charge is 0.1 nC. (c, d): RMS beam size and emittance with the beam charge of 10.0 nC, UV radius of 4.0 mm, matching solenoid current of 240 A.

value of the deviation from the OPAL is 16%(3%) with respect to GPT with adaptive mesh(IMPACT-T). This behavior is now under investigation, and it is expected to be correlated with *NBIN* and number of macroparticles in each cell.

In addition, it is worth noting that, even with the convergence check, it is expected that the trend and final values from those codes would be different due to different calculation algorithm. Therefore, it would be worthwhile to consider some ranges of the tuning parameters to use the simulation results as reference for the experiments.

CSR-Dominated Regime: EEX Beamline

Benchmarking simulations for investigation of the CSR effects between OPAL and IMPACT-T codes have also been performed using EEX beamline. The simulations start just downstream of the mask element; the beam is already cut by the mask and propagates through the EEX line. Final slice distribution after the EEX beamline with different simulation codes are shown in Fig. 4 where Fig. 4(a) shows the initial $(x - y)$ distribution at the entrance of the EEX beamline. After the EEX beamline, the horizontal and longitudinal phase space are exchanged; the bunch longitudinal distribution becomes triangular as shown in Figs. 4(b,c) where all the collective effects are included. Here, there is a slight different slope on the distribution which leads to the difference in terms of the projected density distribution [See Figs. 4(b,c) white solid line]. We found that, even though all the collective effects are not included in the simulation, this slope on the beam still remains. This means that there is a slight different setup of the zero-crossing phase of transverse deflecting cavity.

In addition, even with considering the CSR effects during the simulation, we found that there is no significant changes on the beam distribution compared to that without collective

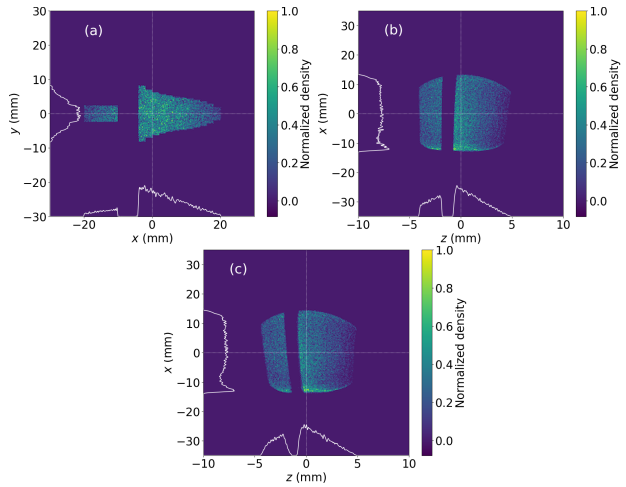

Figure 4: (a): $(x - y)$ distribution after mask. (b, c): $(z - x)$ slice distribution after EEX line from OPAL and IMPACT-T, respectively.

effects. This indicates that the CSR effects are not dominated in this beam case. In both simulation codes, 1D-CSR model [14] with integrated green function method [15] was used. In order to perform the comparison of the beam parameters due to the CSR effects, we need to use the case of the beam where the CSR effects are clearly shown.

CONCLUSION

In this paper, we presented a benchmark of the OPAL simulation results with the results from GPT and IMPACT-T simulations in two cases: in the drive linac and the EEX beamline. In the case of the drive gun with a low space charge force near the cathode, the overall trend and simulation values are reasonably agreed. However, in the case where the space charge force near the cathode is increased, either by using small spot size and short pulse length of the UV with increased beam charge, the OPAL simulation results show that a 0.01 ps timestep is required near the cathode to achieve a reasonable agreement with the other simulation codes. Otherwise, too short of a timestep near the cathode controlled by *EMISSIONSTEPS* gives worse agreement of the RMS envelope and emittance. As a future work, more convergence check will be performed to figure out whether this behavior is closely correlated to the number of energy bins and macroparticles in each cell.

In case of the EEX benchmarking, using the case where the CSR effects are clearly shown in the beam, more systematic investigation on the CSR effects, such as, the analysis of the evolution of the 6D phase space after each dipole magnet will be carried out.

ACKNOWLEDGEMENTS

The computing resources used for this research were provided on BEBOP, a high-performance computing cluster operated by the Laboratory Computing Resource Center (LCRC) at ANL.

ISBN: 978-3-95450-232-5 ISSN: 2673-7000 doi:10.18429/JACoW-NAPAC2022-WEXD5

REFERENCES

[1] N. Neveu, W. Gai, C.-J. Jing, J. Power, and L. Spentzouris, "Staged Two-Beam Acceleration Beam Line Design for the AWA Facility," in *Proc. IPAC'18*, Vancouver, BC, Canada, Apr. 2018, pp. 1688–1691. doi:10.18429/JACoW-IPAC2018-TUPML064

[2] G. Ha, J. G. Power, J. Shao, M. Conde, and C. Jing, "Coherent synchrotron radiation free longitudinal bunch shaping using transverse deflecting cavities," *Phys. Rev. Accel. Beams*, vol. 23, p. 072803, Jul. 2020. doi:10.1103/PhysRevAccelBeams.23.072803

[3] T. Xu *et al.*, "Generation High-Charge of Flat Beams at the Argonne Wakefield Accelerator," in *Proc. IPAC'19*, Melbourne, Australia, May 2019, pp. 3337–3340. doi:10.18429/JACoW-IPAC2019-WEPTS094

[4] G. Ha, M. H. Cho, W. Gai, K.-J. Kim, W. Namkung, and J. G. Power, "Perturbation-minimized triangular bunch for high-transformer ratio using a double dogleg emittance exchange beam line," *Phys. Rev. Accel. Beams*, vol. 19, p. 121301, Dec. 2016. doi:10.1103/PhysRevAccelBeams.19.121301

[5] T. Xu, C.-J. Jing, A. Kanareykin, P. Piot, and J. Power, "Spatio-Temporal Shaping of the Photocathode Laser Pulse for Low-Emittance Shaped Electron Bunches," in *Proc. IPAC'19*, Melbourne, Australia, May 2019, pp. 2163–2166, Jun. 2019. doi:10.18429/JACoW-IPAC2019-TUPTS104

[6] Q. Gao *et al.*, "Observation of high transformer ratio of shaped bunch generated by an emittance-exchange beam line," *Phys. Rev. Lett.*, vol. 120, p. 114801, Mar. 2018. doi:10.1103/PhysRevLett.120.114801

[7] R. Roussel *et al.*, "Single shot characterization of high transformer ratio wakefields in nonlinear plasma acceleration," *Phys. Rev. Lett.*, vol. 124, p. 044802, Jan. 2020. doi:10.1103/PhysRevLett.124.044802

[8] A. Adelmann *et al.*, "Opal a versatile tool for charged particle accelerator simulations," submitted for publication, 2019. doi:10.48550/arXiv.1905.06654

[9] S. B. Van der Geer, O. J. Luiten, M. J. De Loos, G. Poplau, and U. Van Rienen, "3D space-charge model for GPT simulations of high-brightness electron bunches," in *Proc. ICAP'02*, E. Lansing, MI, USA, Oct. 2002, p. 237.

[10] K. Flöttmann *et al.*, "ASTRA: A space charge tracking algorithm," 2011. https://www.desy.de/~mpyflo/

[11] N. Neveu *et al.*, "Benchmark of RF Photoinjector and Dipole Using ASTRA, GPT, and OPAL," in *Proc. NAPAC'16*, Chicago, IL, USA, Oct. 2016, pp. 1194–1196. doi:10.18429/JACoW-NAPAC2016-THPOA46

[12] J. Qiang, S. Lidia, R. D. Ryne, and C. Limborg-Deprey, "Three-dimensional quasistatic model for high brightness beam dynamics simulation," *Phys. Rev. Accel. Beams*, vol. 9, p. 044204, Apr. 2006. doi:10.1103/PhysRevSTAB.9.044204

[13] S. Van Der Geer, O. Luiten, M. De Loos, G. Pöplau, and U. Van Rienen, "3D space-charge model for GPT simulations of high brightness electron bunches," in *Proc. ICAP'02*, E. Lansing, MI, USA, Oct. 2002, p. 101.

[14] E. Saldin, E. Schneidmiller, and M. Yurkov, "On the coherent radiation of an electron bunch moving in an arc of a circle," *Nucl. Instr. Meth. Phys. Res., Sect. A*, vol. 398, no. 2, pp. 373–394, 1997. doi:10.1016/S0168-9002(97)00822-X

[15] C. E. Mitchell, J. Qiang, and R. D. Ryne, "A fast method for computing 1-D wakefields due to coherent synchrotron radiation," *Nucl. Instr. Meth. Phys. Res., Sect. A*, vol. 715, pp. 119–125, 2013. doi:10.1016/j.nima.2013.03.013